Electrodeposition of Rare-Earth Elements from Neodymium Magnets Using Molten Salt Electrolysis

Y. Kamimoto[1*], T. Itoh[2], G. Yoshimura[2], K. Kuroda,[3] T. Hagio[1], R. Ichino[1,3]

[1] Green Mobility Research Institute, Institutes of Innovation for Future Society, Nagoya University, Furo-cho, Chikusa-ku, Nagoya, 464-8603, Japan

[2] Graduated School of Engineering, Nagoya University, Furo-cho, Chikusa-ku, Nagoya, 464-8603, Japan

[3] Institute of Materials and Systems for Sustainability, Nagoya University, Furo-cho, Chikusa-ku, Nagoya, 464-8603, Japan

*Corresponding author: kamimoto@gvm.nagoya-u.ac.jp

Tel: +81-52-747-6595, Fax: +81-52-788-6169

ABSTRACT

Rare-earth element is an important target for recycling in Japan. In our previous work, we demonstrated the selective leaching of rare-earth elements from waste neodymium magnets using chloride molten salt electrolysis. In this study, we investigated the electrodeposition of rare-earth elements using liquid metal as a cathode. The reduction potential obtained using a liquid-zinc electrode was higher than that obtained using a solid molybdenum electrode. A zinc– rare-earth alloy was formed as the electrodeposit. The total rare-earth element content of the electrodeposit was more than 99.8 mass% without zinc and other composition of electrolysis. The activity of rare-earth elements decreased upon alloy formation, suggesting that the oxidation rate of electrodeposited alloy will be decreased.

Keywords: Rare-earth elements, neodymium magnet, electrochemistry, molten salt, liquid zinc electrode

INTRODUCTION

Rare-earth elements are important in industry and are the prime targets for recycling. Rare-earth elements can be recovered as metals from waste materials via a multistage recycling process involving dissolution in acid, solvent extraction, and fluoride molten salt electrolysis. Since all rare-earth elements have similar chemical characteristics, multiple cycles of solvent extraction are required to separate each element. Neodymium magnets, which comprise iron, neodymium, dysprosium, praseodymium, and boron, contain a primary phase ($Nd_2Fe_{14}B$ alloy) and a boundary phase (rare-earth metals). Dysprosium, which is more expensive than neodymium and praseodymium, is added to the boundary phase of neodymium magnets to improve their heat resistance. Several methods for the recovery of rare-earth elements have been developed, including hydrometallurgical treatment [1-3], hydrothermal processing [4], molten metal extraction [5-7], molten salt extraction [8], chloride volatility processing [9], and glass slag processing [10]. These processes recover rare-earth oxides, which then have to be reduced to metals via molten salt electrolysis. We have reported the leaching of rare-earth elements from neodymium magnets using molten salt electrolysis [11], in which rare-earth elements were recovered as alloys on a solid cathode [12]. Using our process, rare-earth alloys can be recovered from neodymium magnets via a single molten salt electrolysis process. Although it was low adhesion between cathode (molybdenum and carbon) and electrodeposition (rare-earth alloy), rare-earth alloy separates easily from cathode into molten salt. The adhesion between cathode electrode and electrodeposition is increased with the formation of intermetallic compounds. Intermetallic compounds are suitable material for electrowinning process because it is difficult to collect target materials and elements from intermetallic compounds. Zinc, which is a high-vapor-pressure metal, forms alloys with many elements, and critical materials is separated from the zinc alloy using distilling process [13].And the activity of rare-earth elements decreases upon alloy formation, thereby delaying their oxidation.

In this study, we examine the electrodeposition of rare-earth elements from neodymium magnets on a liquid metal cathode via molten salt electrolysis. We optimized the electrodeposition conditions based on the cathode polarization curves and cyclic voltammograms and investigated the electrodeposition behaviors of various rare-earth elements.

MATERIALS AND METHODS

Experimental equipment

The experimental apparatus used for electrochemical examinations is shown in Fig. 1. The electrolysis potential was controlled using a potentiostat (HZ-5000; Hokuto Denko). The reactor was made of Pyrex glass and purged with Ar gas. A eutectic salt mixture of 59 mol% LiCl and 41 mol% KCl, which melted at 723 K, was used to fill the electrolysis bath. The cathode and working electrode were zinc and molybdenum, respectively, Zinc was in liquid metal form. Liquid zinc was placed in a glass petri dish and connected with an electric circuit to detect electrochemical behavior using a tungsten wire coated with a glass film. The anode and counter electrode for cathodic polarization and cyclic voltammetry were glassy carbon rods. In potentiostatic electrolysis experiments, the neodymium magnet anode was placed in a tantalum-plate bucket to avoid diffusion of magnet residue to the electrolyte. The magnet was cut to dimensions of $5 \times 5 \times 2$ mm^3,

and the weight of each magnet was 1 g. The nickel coating on each neodymium magnet was removed before electrolysis. The reference electrode was a Ag/AgCl (0.1 mol%) electrode in a eutectic LiCl–KCl mixture; this electrode was placed in a mullite tube. The electrolysis bath was maintained at 473 K for 24 h under vacuum to eliminate water.

Analytical method

The compositions of the neodymium magnet, electrolysis bath, anodic residues, and electrodeposited materials were analyzed via inductively coupled plasma-atomic emission spectrometry (ICP-AES; Optima-3300DV, PerkinElmer). Samples for ICP-AES analysis were dissolved in aqua regia. The surface morphologies of the samples were observed via scanning electron microscopy (SEM; JSM-6330F, JEOL). The electron microscope was equipped with an energy-dispersive X-ray spectrometer. The electrodeposited products were identified using X-ray diffraction (XRD) via a diffractometer (XRD-6100, Shimadzu).

The current efficiency (C_{eff}) was calculated from the composition change of the neodymium magnet, with detected by ICP-AES using the following equation:

$$C_{eff} = \frac{(Z_{Nd} n_{Nd} F + Z_{Pr} n_{Pr} F + Z_{Dy} n_{Dy} F)}{Q}$$

where Z_X represents the charge of each element; n_X is the molar amount obtained from the ICP analysis of each element; F is the Faraday constant; Q is the quantity of electricity; and X represents either neodymium, praseodymium, or dysprosium.

RESULTS AND DISCUSSION

Cathodic polarization

The cathodic polarization scanning rate was 5 mV s^{-1}, and 1.4 mol% $NdCl_3$, $DyCl_3$, $FeCl_2$ were added to electrolyte for analysis of each cathodic polarization curves. Neodymium, dysprosium and iron are main component of in neodymium magnet. The cathodic polarization curves on the liquid zinc electrode are shown in Fig. 2. The reduction currents of neodymium and dysprosium were generated at approximately −1.6 V, and their reduction potentials were lower than that of iron. The reduction potential of lithium was the lowest in this condition. If lithium is reduced on the cathode, it will reduced rare-earth elements by immersion reaction. Since lithium was reduced to metal in the early period, it is suggested that reduction of lithium does not decreased current efficiency of this process.

Electrochemical behavior of rare-earth elements on the liquid-zinc electrode

The scanning rate for cyclic voltammetry was 50 mV s^{-1}, and 1.4 mol% $NdCl_3$ was added to the electrolyte. The cyclic voltammograms for the solid molybdenum and liquid-zinc electrodes are shown in Fig. 3. Neodymium and lithium were respectively reduced at approximately −2.2 and −2.6 V on the solid molybdenum electrode, and reduced neodymium and lithium were respectively oxidized at approximately −2.0 and −2.3 V. On the liquid-zinc electrode, reduction currents were generated at approximately −1.9, −1.5, and −1.0 V, and the corresponding oxidation currents were found at −2.0, −1.5, and −1.1 V, respectively. The

lower-potential reaction on the molybdenum electrode was attributed to the oxidation and reduction of lithium. The lower potentials on the liquid-zinc electrode corresponded to the oxidation and reduction of neodymium. The reduction potential of neodymium was higher on the liquid-zinc electrode than on the molybdenum electrode. The reduction current on molybdenum was consumed by neodymium electrowinning and that on liquid zinc was consumed by the formation of zinc–neodymium alloy. The reduction currents on the liquid-zinc was respectively generated at approximately −1.5 and −1.2 V, there are consumed by neodymium−zinc alloy. The reduction potential on the alloy electrode was greater than that of the unalloyed metal. These results indicate that the liquid-zinc electrode was suitable for the reduction of rare-earth elements.

Potentiostatic reduction

Previous studies using potentiostatic electrolysis demonstrated that rare-earth elements are selectively leached from neodymium magnets. There were shown that the contents of rare-earth elements of neodymium magnets electrolyzed at an electrolysis potential of −1.0 V and a quantity of electricity of 830 C decreased to 2.0%, and the estimated leaching ratio of rare-earth elements was approximately 90% [11-12]. Table 1 shows the elemental compositions of the neodymium magnet, the electrolyzed neodymium magnet, the molten salt, and the electrodeposit. The total rare-earth element content of the electrodeposit was more than 99.8 mass%. The surface XRD pattern of the electrolyzed zinc cathode is shown in Fig. 4. The corresponding elemental composition of electrodeposit layer is shown in Fig. 5. During the electrolysis process, the weight of the neodymium magnet decreased by 0.375 g. Neodymium ion was leached as a trivalent cation from the neodymium magnet. The current efficiency of rare-earth elements was calculated as 91.5%. Based on XRD analysis, the electrodeposit contained a zinc– rare-earth alloy, rare-earth oxides, and rare-earth oxychlorides. Rare-earth oxychlorides were synthesized quickly and easily from the rare-earth metals in the presence of oxygen and chloride, and rare-earth oxides were done from rare-earth metals in the presence of oxygen.

The electrodeposit on the zinc cathode was high adhesion layer. The electrodeposit formed a spherical and acicular cluster, which was identified by SEM-EDX to comprise rare-earth element–zinc alloy. The thickness of rare-earth elements–zinc alloy was 3 μm. The rare-earth elements content is increased with thickness of the electrodeposited layer. The reduction potential of an alloy is greater than that of the corresponding pure metal, it was suggested that reduction current increased with increasing reduction potential from ion to metals on alloy electrode.

CONCLUSION

Rare-earth elements were reduced to alloys and metals using molten salt electrolysis. The reduction potential on the liquid-zinc cathode was higher than that on the solid molybdenum cathode and decreased upon alloy formation. The rare-earth elements were leached from a neodymium magnet at −1.0 V; the leached rare-earth elements were simultaneously reduced to metals on the cathode electrode, and alloys made of zinc and rare-earth metals were formed. The electrodeposit contained more than 99.8 mass% of rare-earth elements. The rare-earth element content of the alloy decreased moving from the edges towards the interior.

The current efficiency of the rare-earth elements leaching was calculated to be 91.5%.

Acknowledgments This work was supported by the Environment Research and Technology Development Fund of the Ministry of the Environment, Japan 3K143005, JSPS KAKENHI Grant Number 24656457, Japan Oil, Gas and Metals National Corporation, the Hori Sciences and Arts Foundation, and the Tokai Foundation for Technology.

REFERENCES

[1] Rabatho JP, Tongamp W, Takasaki Y, Haga K, Shibayama A (2013) Recovery of Nd and Dy from rare earth magnetic waste sludge by hydrometallurgical process. J. Mater. Cycles Waste Manag. 15: 171-178

[2] Hoogerstraete TV, Wellens S, Verachtert K, Binnemans K (2013) Removal of transition metals from rare earths by solvent extraction with an undiluted phosphonium ionic liquid: separations relevant to rare-earth magnet recycling. Green Chem. 15: 919-927

[3] Kikuchi Y, Matsumiya M, Kawakami S (2014) Extraction of Rare Earth Ions from Nd-Fe-B Magnet Wastes with TBP in Tricaprylmethylammonium Nitrate. Solv. Extr. Res. Dev. Jpn. 21:137-145

[4] Itakura T, Sasai R, Itoh H (2006) Resource recovery from Nd–Fe–B sintered magnet by hydrothermal treatment. J. Alloy Compd. 408-412: 1382-1385

[5] Takeda O, Okabe TH, Umetsu Y (2006) Recovery of neodymium from a mixture of magnet scrap and other scrap. J. Alloy Compd. 408-412: 387-390

[6] Sekimoto H, Kubo T, Yamaguchi K (2014) Development of a New Recycling Process for Neodymium Permanent Magnet Using B2O3 Flux (in Japanese). J. MMIJ. 130: 494-500

[7] Hoshi H, Miyamoto Y, Furusawa K (2014) Technique for Separating Rare Earth Elements from R-Fe-B Magnets by Carbothermal Reduction Method (in Japanese). J. Japan Inst. Met. Mater. 78: 258-266.

[8] Takeda O, Nakano K, Sato Y (2014) Recycling of Rare Earth Magnet Waste by Removing Rare Earth Oxide with Molten Fluoride. Mater. Trans. 55: 334-341

[9] Itoh M, Miura K, Machida K (2009) Novel rare earth recovery process on Nd–Fe–B magnet scrap by selective chlorination using NH_4Cl. J. Alloy Compd. 477: 484-487

[10] Saito T, Sato H, Ozawa S, Yu J, Motegi T (2003) The extraction of Nd from waste Nd–Fe–B alloys by the glass slag method. J. Alloy Compd. 353: 189-193

[11] Kamimoto Y, Yoshimura G, Itoh T, Kuroda K, Ichino R (2016) Recovery of rare-earth elements from neodymium magnets using molten salt electrolysis. J. Mater. Cycles Waste Manage. 19: 1017-2021

[12] Kamimoto Y, Yoshimura G, Itoh T, Kuroda K, Ichino R (2015) Leaching of Rare Earth Elements from Neodymium magnet using Electrochemical method. Trans. Mat. Res. Japan 40: 343-346

[13] Okabe TH, Takeda O, Fukuda K, Umetsu Y (2003) Direct Extraction and Recovery of Neodymium Metal from Magnet Scrap. Mater. Trans. 44: 798-801

TABLE CAPTIONS

Table1 Elemental compositions of the neodymium magnets, electrolyzed residual magnet, electrolyzed molten salt, and electrodeposit in this study (mass%)

FIGURE CAPTIONS

Fig. 1 Experimental apparatus.

Fig. 2 Cathode polarization curves of (1) neodymium, (2) dysprosium, (3) iron, and (4) lithium.

Fig. 3 Cyclic voltammograms for solid molybdenum and liquid-zinc electrodes.

Fig. 4 XRD pattern of the zinc cathode during the controlled-potential electrolysis process.

Fig. 5 Composition of the electrodeposit in cross section direction (mol%)

Table1 Elemental compositions of the neodymium magnets, electrolyzed residual magnet, electrolyzed molten salt, and electrodeposit in this study (mass%)

	Nd	Dy	Pr	Fe	B	Al
Neodymium magnet	18.0	9.7	3.9	67.0	0.8	0.5
Residual	2.4	1.5	0.2	94.0	1.3	0.6
Molten salt	55.5	38.9	5.0	0.6	0	0.4
Electrodeposit	57.0	40.8	1.8	0.2	0	0.2

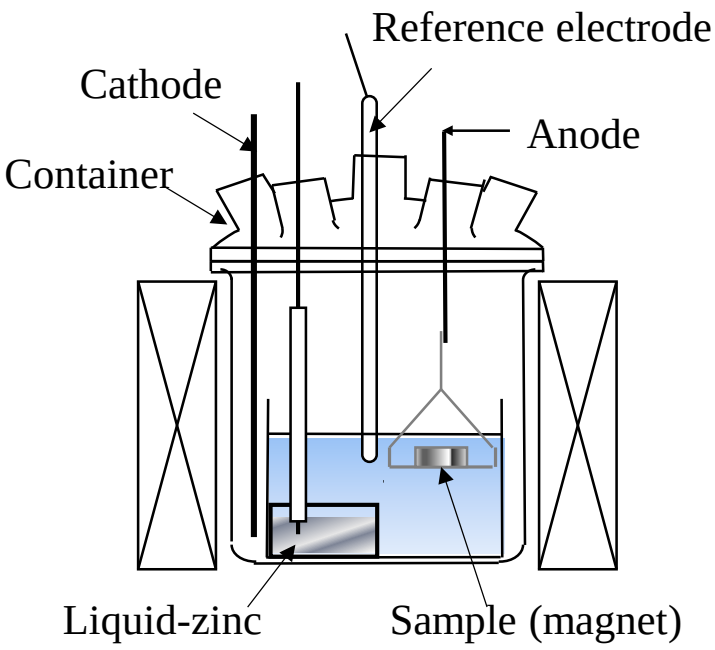

Fig. 1 Experimental apparatus

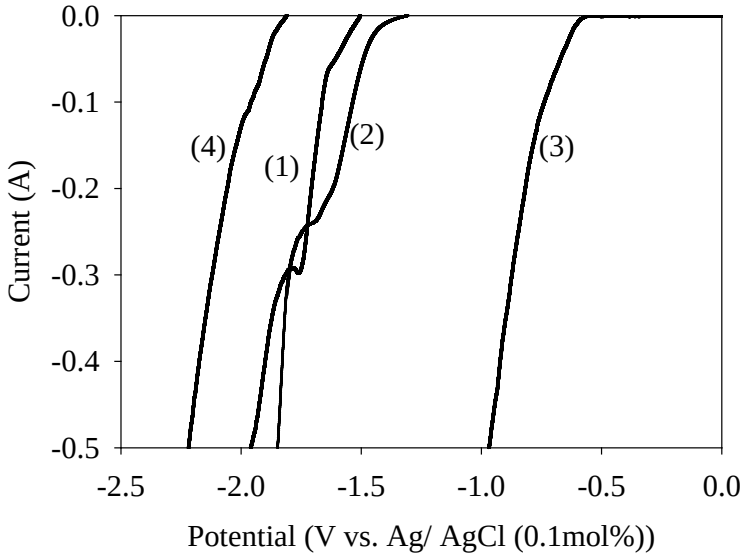

Fig. 2 Cathode polarization curves of (1) neodymium, (2) dysprosium, (3) iron, and (4) lithium.

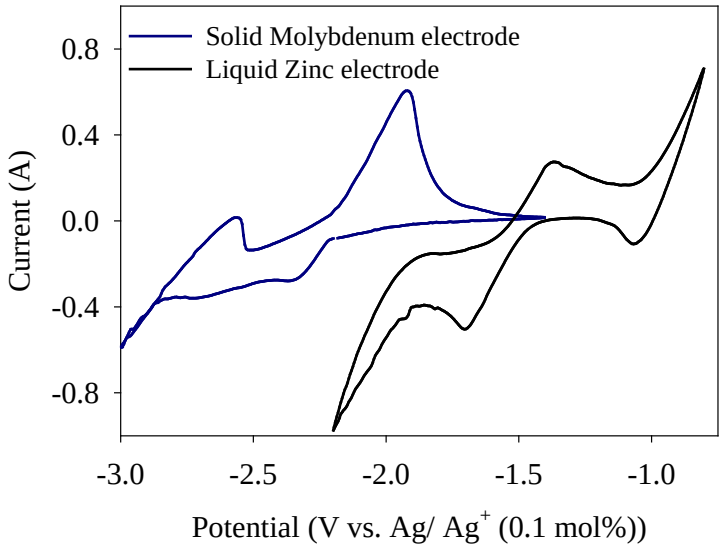

Fig. 3. Cyclic voltammograms for solid molybdenum and liquid-zinc electrodes.

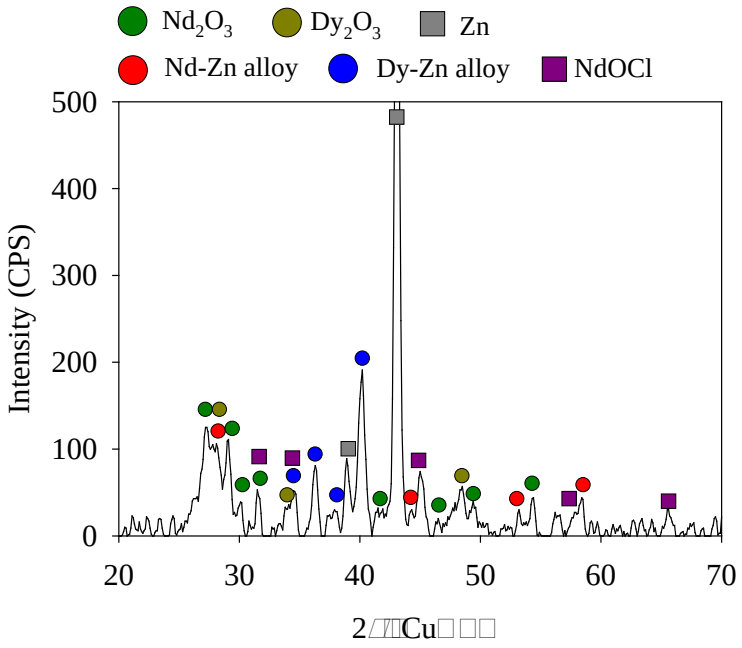

Fig. 4 XRD pattern of the zinc cathode during the controlled-potential electrolysis process.

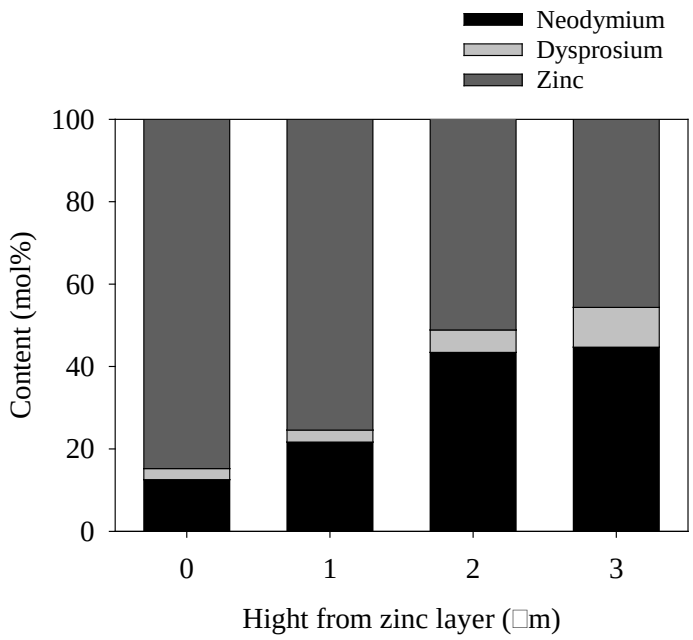

Fig. 5 Composition of the electrodeposit in cross section direction (mol%)